RSC Advances

PAPER

Cite this: *RSC Adv.*, 2022, **12**, 27380

Synthesis of linear and star-shaped telechelic polyisobutylene by cationic polymerization†

Zhaopeng Yu, Xiaohu Feng, Chenqi Zhao, Jiajun Li, Ruofan Liu, Yushun Jin* and Yibo Wu *

Received 21st July 2022
Accepted 9th September 2022

DOI: 10.1039/d2ra04504d

rsc.li/rsc-advances

Hydroxyl-terminated linear and star-shaped telechelic polyisobutylene have been successfully synthesized by living cationic polymerization using propylene oxide (PO)/Titanium tetrachloride ($TiCl_4$) as the initiator system. A one-step method to prepare the terminal hydroxyl group was realized by selecting the cheap and beautiful epoxide as the functional initiator, which has the prospect of industrial application. The polymerization mechanism was proposed by the end structure analysis and Gaussian calculation results. At the same time, the living linear macromolecular chain was used as the starting point to react with divinyl compounds for synthesis of star-shaped hydroxyl-terminated polyisobutylene. The effects of initiator-crosslinking agent ratio, arm length, and reaction time on the coupling reaction were studied.

1 Introduction

Polyisobutylene (PIB) is a very useful macromolecular raw material and synthetic intermediate prepared by cationic polymerization. It shows excellent low-temperature flexibility, thermal stability, hydrolytic stability, chemical resistance, hydrophobicity, and gas tightness. Isobutylene is usually copolymerized with isoprene to prepare butyl rubber in industry.[1–3] PIB and its derivatives have also been applied in the biomedical materials field due to their excellent biocompatibility; PIB block copolymers have been used for coronary stent coating and glaucoma catheters due to their excellent biocompatibility.[4–9]

Liquid rubber is a kind of oligomer of viscous liquid at room temperature. Usually, the number average molecular weight of liquid rubber is between 500 and 10 000 g mol^{-1}. The viscosity of liquid rubber varies with the molecular weight and molecular configuration of the polymer. Compared with traditional commercial rubbers, liquid rubber has the advantages of good fluidity, being easy-to-process and the possibility of continuous production. Thus, liquid rubber was called the "new generation of gold rubber". Functionalized liquid rubber is widely used as a macromolecular raw material, plasticizer and crosslinker.[10–15] However, it is not easy to prepare liquid PIB rubber. The traditional PIB has a totally saturated backbone structure, without any modifying groups. Thus, to achieve liquid PIB rubber, functionalized telechelic structure is the only possible method so far.[16–32]

Kennedy is the first researcher to report the synthesis of hydroxyl-terminated PIB liquid rubber.[33,34] Firstly, PIB with the end of tertiary chlorine was synthesized by using the difunctional initiator/BCl_3 as the initiator system. Then the allyl end was generated by removing HCl from the chain ends. Finally, hydroxyl-terminal polyisobutylene was prepared by borohydride oxidation reaction.[35,36] Followed that, Faust *et al.* synthesized hydroxyallyl telechelic PIB through the hydrolysis of chloroallyl telechelic PIB, which derived from living PIB end-capped with 1,3-butadiene.[37,38] Subsequently, the group utilized thiol–ene click chemistry to produce HO–PIB–OH.[39] Wu *et al.* provided a new idea.[40] The hydroxy-telechelic PIB was successfully synthesized by the combination of capping and hydrolysis.

However, all of the previous methods require complex experimental procedures and harsh reaction conditions. For examples, the borohydride/oxidation reaction takes a long time; the reagent is expensive; and the chemical hydrolysis process requires extremely dilute solution. Recently, Puskas *et al.* reported that the carbocationic polymerization of isobutylene (IB) was initiated by epoxy compounds with substituents. They also successfully synthesized PIB with hydroxyl structure at the head and proposed a competitive reaction mechanism.[41]

Star-branched polymers have attracted wide attention because of their lower solution viscosity and bulk viscosity. They not only have multi-arm chains, end groups, and intramolecular functional space but also allow enough entanglement between arm chains.[42,43] Thus, they give a good advantage in the material processing. Therefore, if we can quantitatively synthesize star-shaped telechelic PIB with a specific structure, it can greatly improve the application area of the possible new materials with network structure.

The College of New Materials and Chemical Engineering, Beijing Key Lab of Special Elastomer Composite Materials, Beijing Institute of Petrochemical Technology, Beijing 102617, China. E-mail: wuyibo@bipt.edu.cn; jinyushun@bipt.edu.cn

† Electronic supplementary information (ESI) available. See https://doi.org/10.1039/d2ra04504d

Among various methods for preparing telechelic polymers, the functional initiator initiation method is undoubtedly the most convenient one. In this study, the living cationic polymerization of IB was achieved by the PO/$TiCl_4$ initiator system, and the linear hydroxyl-terminated PIB with a clear structure was synthesized successfully. On this basis, the feasibility of rapid and quantitative synthesis of star-shaped hydroxyl-terminated PIB by cationic polymerization was investigated. The effects of initiator-crosslinking agent ratio, arm length, and reaction time on the coupling reaction were studied. This preparation method has the advantages of cheap raw materials and a simple synthesis route, which gives it potential industrial usability.

2 Experimental

2.1 Materials

Methyl chloride (MeCl) (99.5%; Beijing Yanshan Petroleum Chemical Co.), isobutylene (IB) (99.9%; Beijing Yanshan Petroleum Chemical Co.), and 2,6-di-*tert*-butylpyridine (DtBP) (96%, J&K Scientific Ltd) were used as received. Titanium tetrachloride ($TiCl_4$) (99%; J&K Scientific Ltd) was dried using phosphorus pentoxide (P_2O_5) under N_2 atmosphere before use. *n*-Hexane (Hex) (99.5%; Beijing Yanshan Petroleum Chemical Co.) was distilled twice by using CaH_2 under N_2 atmosphere before use. Propylene oxide (PO) (99.5%; J&K Scientific Ltd) was distilled prior to use. Divinylbenzene (DVB) (80% in EVB + DEB, J&K Scientific Ltd) were purified through vacuum distillation.

2.2 Preparation of linear telechelic PIB

The whole polymerization was carried out under a dry N_2 atmosphere in an MBraun glove box. A typical example preparation was given as follows. A certain volume ratio of Hex/MeCl solvent mixtures was used as reaction solvent at −80 °C. IB, PO and DtBP were added to the solvent in a three-necked flask. The polymerization was started by the addition of the co-initiator $TiCl_4$. The reaction mixture was stirred at 150 r min^{-1} throughout the polymerization. After 30 minutes reaction time, the reaction was terminated by adding pre-cooled methanol. Then the product was transferred to a fume hood overnight to evaporate the solvent. Next, the polymer was purified with hexane/ethanol several times to remove initiators and monomers. Finally, the product was dried to a constant weight in a vacuum oven (50 °C) to obtain liner telechelic PIB (PIB–OH). The conversion rate was determined by weight difference method.

2.3 Preparation of star-shaped telechelic PIB

The early stage of the synthesis is the same to prepare liner telechelic PIB. When monomer IB had consumed almost quantitatively by living cationic polymerization, the divinylbenzene compound was added to reaction mixture. The reaction was quenched with pre-cooled methanol. The same method was used for post-treatment of polymer.

2.4 Characterization

The chemical structure of the polymer was determined by a Bruker-500 MHz ^{1}H-NMR. $CDCl_3$ was chosen as the solvent. The concentration of the polymer was 6 mg mL^{-1} with tetramethylsilane (TMS) as the internal standard.

The molecular weight and molecular weight distribution of the polymer were determined by a GPC system (Wyatt Co. USA). It includes a multi-angle laser scattering instrument (MALLS), a viscometer, and a differential refractive index detector (RI). THF was used as the mobile phase, and the flow rate was 1 mL min^{-1}. Samples were put in a tube with THF and was shaken for more than 8 h at 40 °C water bath to fully dissolve before the tests.

FT-IR tests was completed by Fourier transform infrared spectrometer (Nicoloet 380, USA). The product was dissolved in anhydrous dichloromethane. Then the solution was coated to potassium bromide wafer. The test was used by an FT-IR analyzer with a scan range of 4000–400 cm^{-1}, 64 scans, and a resolution of 2 cm^{-1}.

Differential scanning calorimeter (DSC; Q2000, USA) was operated to determine the glass transition temperature (T_g) in the range from −90 to 10 °C for product polymers. The heating and cooling rates were 10 °C min^{-1}.

TG tests was carried out with a thermal gravimetric analyzer (Q500, USA). The decomposition temperature was tested at the rate of 10 °C min^{-1} from room temperature to 550 °C under N_2 atmosphere.

The average number of arms per star-shaped polymer (N) were calculated using the following equation:[44]

$$N = \frac{\text{Mw of star shaped polymer} \times \text{weight fraction of arm segment}}{\text{Mw of linear polymer(arm presursor)}}$$

$$\text{weight fraction of arm segment} = \frac{\text{monomer weight}}{\text{monomer weight} + \text{DVB weight}}$$

3 Results and discussion

3.1 Synthesis of linear telechelic PIB

The polarity of the solvent has great influence on the cationic polymerization rate. The solvent has low polarity, causing ion pairs to have difficult dissociation that tend to form tight ion pairs. Thus, the reaction rate becomes slow. On the contrary, with the increase in solvent polarity, ion pairs tend to form free ions, thereby resulting in uncontrolled polymerization. Therefore, A series of solvents, from polar to non-polar, has been used to determine the most suitable solvent to the synthesis.

As shown in Fig. 1a, monomer conversion was highest when the volume ratio of non-polar solvent (hexane) to polar solvent (MeCl) was 6 : 4. From Fig. 1b, the polymer molecular weight distribution was narrowest when the volume ratio of hexane to MeCl was 6 : 4. However, the reduced initiation efficiency leads

to a larger molecular weight of the polymer. This may be due to the low solvent polarity, which inhibits the ring-opening initiator efficiency of epoxides. Depending on that, one can conclude that the volume ratio of Hex and MeCl in the IB cationic polymerization should be 6 : 4. At this ratio, the cation living centers can be stabilized, and side reactions, such as chain transfer reaction, can be avoided. The following experiments are based on this result.

After determining the composition of the reaction solvent, in order to study the efficiency of PO/$TiCl_4$ system to initiate IB living cationic polymerization. We explored the relationship of reaction time with polymer molecular weight. A series of products under the same reaction conditions with different reaction time has been synthesized. It can be clearly observed from Fig. 2a that with the extension of polymerization time, the elution time of the differential curve continues to move forward,

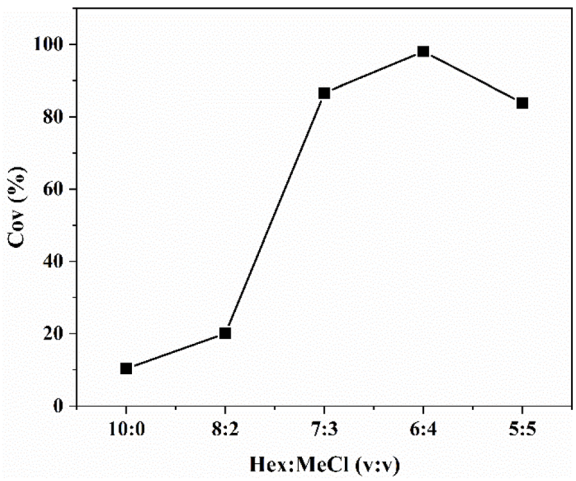

(a)

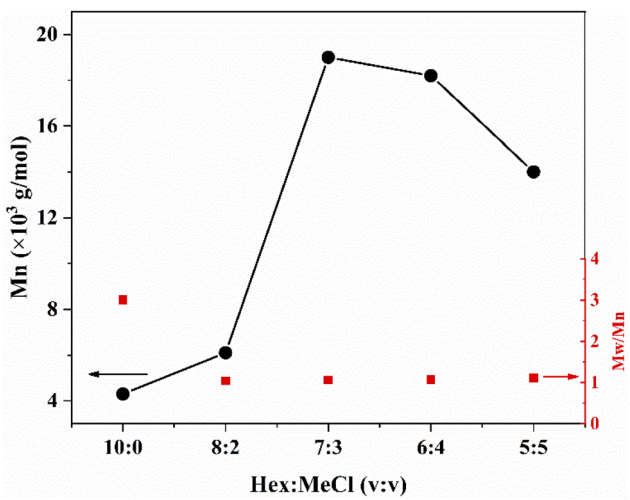

(b)

Fig. 1 (a) Effect of solvent polarity on monomer conversion; (b) effect of solvent polarity on molecular weight and molecular weight distribution. Reaction conditions: $T = -80$ °C, [PO] = 0.039 M, [$TiCl_4$] = 0.078 M, [DTBP] = 0.01 M, [IB] = 3.38 M, reaction time = 60 min.

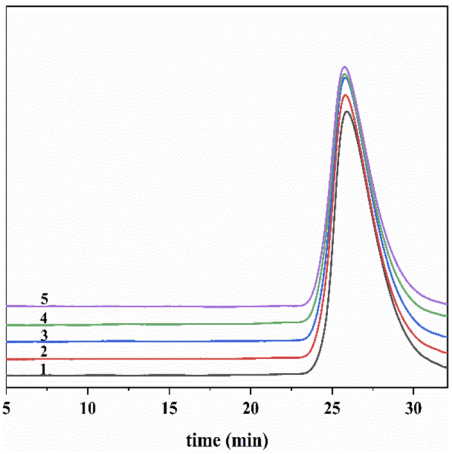

(a)

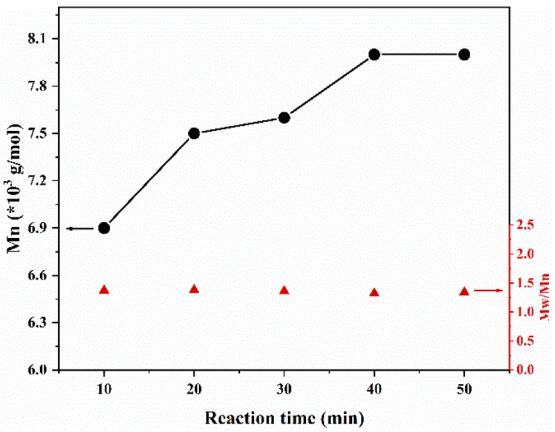

(b)

Fig. 2 (a) RI signal as a function of elution time of products; (b) relationship between reaction time and molecular weight, molecular weight distribution. Reaction conditions: $T = -80$ °C, [PO] = 0.09 M, [$TiCl_4$] = 0.18 M, [DTBP] = 0.01 M, [IB] = 3.38 M, Hex/MeCl = 6/4 (v/v), reaction time 1–10 min, 2–20 min, 3–30 min, 4–40 min, 5–50 min.

indicating the molecular weight increased. All the differential elution curves of the polymer show symmetrical narrow unimodal distribution. It can be seen from Fig. 2b that the molecular weight of the polymer has reached the maximum at the reaction time of 30 min. over that, with the extension of the reaction time, the changes of molecular weight are neglectable. The molecular weight distribution of the polymer kept at a narrow level. Therefore, the reaction can be terminated rapidly when the polymerization time is 30 min. It also proves that the PO/$TiCl_4$ system can initiate IB living cationic polymerization.

On the basis of appropriate solvent ratio and reaction time, experiments can be designed to achieve the one-step preparation of different molecular weight products. Fig. 3 shows the RI signal as a function of elution time of various products. All curves showed symmetrical narrow distribution. Fig. 4 shows the light scattering intensity as a function of elution time of the product, and no impurity peaks appear. Laser and differential

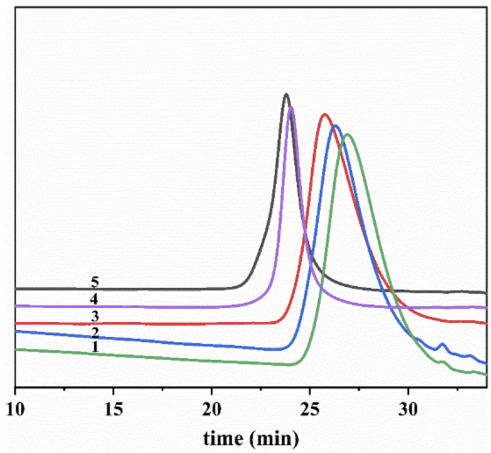

Fig. 3 RI signal as a function of elution time of products. Reaction conditions: $T = -80$ °C, $[TiCl_4]$: [PO] = 2 : 1, [DTBP] = 0.01 M, [IB] = 3.38 M, Hex/MeCl = 6/4 (v/v), reaction time = 30 min, 1-[PO] = 0.21 M, 2-[PO] = 0.15 M, 3-[PO] = 0.09 M, 4-[PO] = 0.05 M, 5-[PO] = 0.02 M.

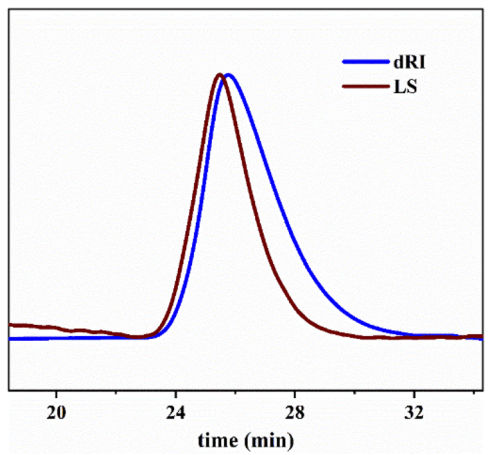

Fig. 4 Light scattering intensity as a function of elution time. Reaction conditions: $T = -80$ °C, [PO] = 0.09 M, $[TiCl_4]$ = 0.18 M, [DTBP] = 0.01 M, [IB] = 3.38 M, Hex/MeCl = 6/4 (v/v), reaction time = 30 min.

curve trace agree with each other. They both indicate that the initiation system has high dissociation degree. The chain initiation process is uniform, which can achieve the synchronous chain growth.

Table 1 shows the molecular weight and molecular weight distribution data that correspond to the Fig. 3. The molecular weight distribution of the product is narrow, while the conversion rate is high. We found that increasing the [IB]/[PO] ratio increased initiator efficiency (I_{eff}). It indicates that the one-step synthesis of hydroxyl-terminated PIB with different molecular weight can be achieved by PO initiation system living cationic polymerization.

Next, we characterized the polymer structure by FT-IR and ^{1}H-NMR. The FT-IR spectrum of the polymers in Fig. 5 reveal the hydroxyl (–OH) absorption at 3350 cm^{-1}; the –C–O absorption at 1052 cm^{-1}; the stretching vibration of –C–H absorption at 2950 cm^{-1} and 2890 cm^{-1}; and the bending vibration of –CH

Table 1 Molecular weight data corresponding to elution curve[a]

Run	PO (M)	Mn (g mol^{-1})	Mw/Mn	Conv. (%)	I_{eff} (%)
1	0.21	4548	1.30	89	19.5
2	0.15	6000	1.25	92	21.3
3	0.09	8100	1.22	90	25.6
4	0.05	12 500	1.21	88	32.9
5	0.02	28 000	1.16	93	34.8

[a] Reaction conditions: $T = -80$ °C, $[TiCl_4]$: [PO] = 2 : 1, [DTBP] = 0.01 M, [IB] = 3.38 M, Hex/MeCl = 6/4 (v/v), reaction time = 40 min.

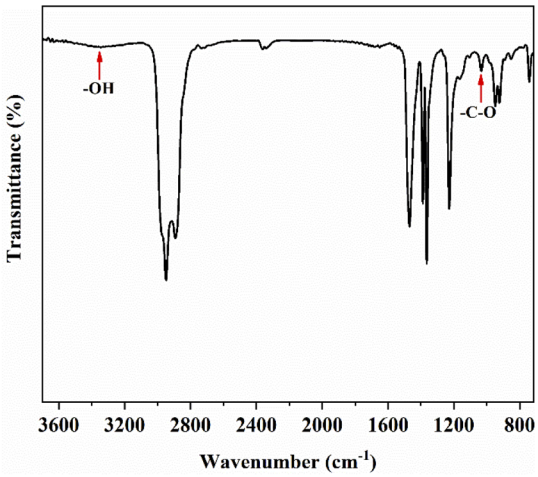

Fig. 5 FT-IR spectrum of PIB–OH.

absorption at 1460 cm^{-1} and 1365 cm^{-1}. Hydroxyl-terminated PIB was successfully synthesized.

Fig. 6 shows the ^{1}H-NMR spectrum of PIB–OH. The characteristic resonances at $\delta = 1.10$ ppm (peak d) and $\delta = 1.42$ ppm (peak c) were assigned to the methyl and methylene groups of IB, respectively. The proton resonances at $\delta = 3.31$ ppm (peak a′) and $\delta = 3.48$ ppm (peak a) correspond to the methylene protons that are next to the primary hydroxyl head group, and these two protons split because the neighboring protons are chiral. Calculated from the ratio of the integral of the CH_2 proton signals next to the OH at $\delta = 3.31$ ppm (b) to that of the backbone methylene protons at $\delta = 1.42$ ppm (c), the molecule weight of the polymer can been determined as 3979 g mol^{-1}. The result is in excellent agreement with Mn = 3996 g mol^{-1} from MALLS. These results indicated the synthesis of functionalized PIB with well-defined structure and quantitative hydroxyl group.

As an explanation, the main initiator PO follows the SN1 ring opening mechanism after being attacked by Lewis acid $TiCl_4$, thereby forming a living center to initiate polymerization. We compared the charge change and bond length change before and after the coordination of $TiCl_4$ and PO by Gaussian simulation. All density functional theory (DFT) calculations were performed using Gaussian 09 program at the B3LYP/6-31G (d) level. The molecular structure was optimized, and the frequency was calculated. The natural bond orbital (NBO) was analyzed. In the calculation, all the units of bond length are Å.

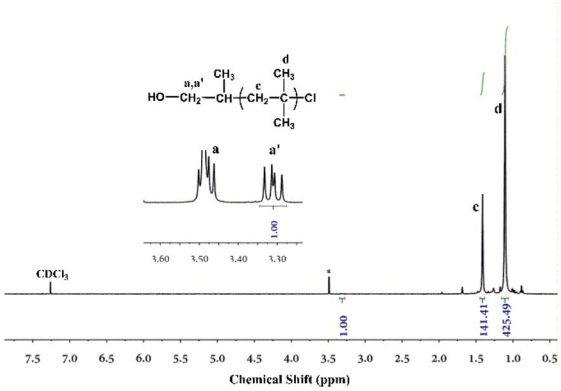

Fig. 6 ^{1}H-NMR spectrum of PIB-OH.

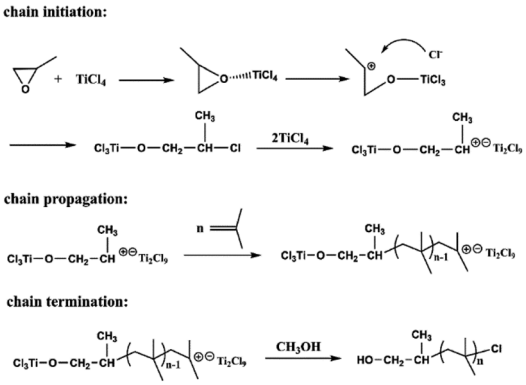

Fig. 8 Postulated reaction mechanism for cationic polymerization of IB using the PO/$TiCl_4$ initiating system.

Fig. 7a shows the simulated structure of PO, and Fig. 7b shows the form of initiator complexation. The results are summarized in Table 2. The bond length of the C_1–O_3 bond attached to the methyl substituent changes when PO undergoes coordination interaction with $TiCl_4$. Its bond length is significantly elongated, increasing from 1.435 Å to 1.462 Å. Therefore, the C_1–O_3 bond, which subsequently promotes the breakage of the C–O bond, is activated. Meanwhile, the NBO analysis shows that the positive charge of the C_1 atom attached to the methyl substituent increases after the coordination of $TiCl_4$ and PO. It reflects a stronger positive charge. This phenomenon also contributes to the formation of a carbocation living center and subsequently initiate the monomer reaction. The above shows that the coordination effect of Lewis acid $TiCl_4$ not only increases the electrophilicity of C_1 but also activates the C–O bond between C_1 and O_3. This finding is consistent with the mechanism of ring-opening initiated polymerization later.

According to the above research results, the IB polymerization mechanism can be drawn (Fig. 8). $TiCl_4$ is a Lewis acid. In this system, it act as an electrophilic reagent, and a strong oxyphilic reagent. When $TiCl_4$ is added to the system, it will attack the initiator PO to form Ti–O covalent bond. This approach also accelerates the breakage of the adjacent C–O bonds. Then the epoxide is attacked by Lewis acid, following the SN1 ring-opening mechanism. Thus, the carbon atoms attached to the methyl substituent undergo the breaking down of C–O bonds and gain positive charges. Then, $TiCl_4$ also breaks the Ti–Cl bond, allowing the chloride ion to combine with the carbon ion to form C–Cl covalent bonds. At the same time, the $TiCl_4$ and this compound form complex ion pairs into the equilibrium state. Next, the pairs would combine with a IB monomer that forms a living cationic reaction center to initiate polymerization. Then, the chain propagation stage begins. Moreover, the Ti–O bonds decomposed during the quenching reaction with methanol, which led to the generation of a hydroxy group at the α-end.

In order to compare with traditional PIB, the thermal properties of telechelic PIB has been characterized. The thermal analysis of the polymer was tested using heat flow-type DSC, specifying upward as the direction of exothermic effect. As shown in Fig. 9, the glass transition temperature (T_g) of PIB–OH is −66.8 °C. The hydroxy-terminated PIB product has excellent low-temperature properties.

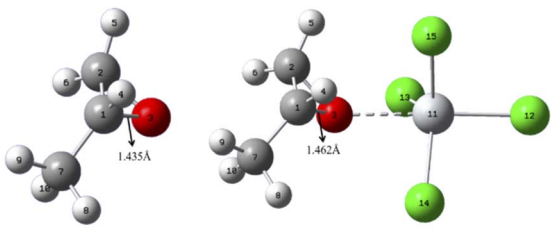

(a) PO (b) PO-$TiCl_4$

Fig. 7 Schematic diagram of the structure changes of PO after adding $TiCl_4$.

Table 2 Gaussian data analysis

Name	C_1–O_3 bond length (Å)	NBO charge (C_1)
PO	1.435 Å	0.05229
PO-$TiCl_4$	1.462 Å	0.07299

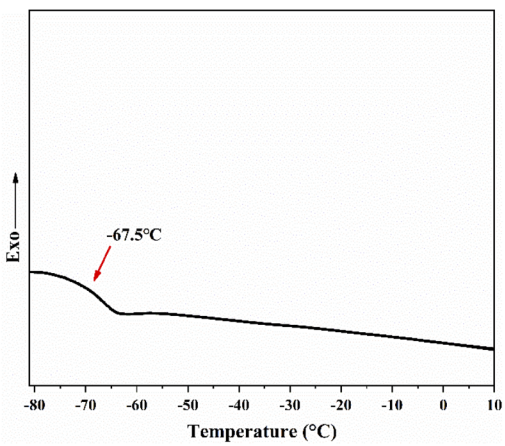

Fig. 9 DSC curve of PIB–OH.

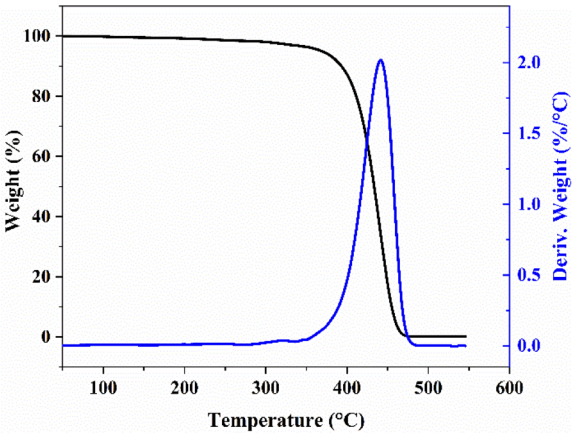

Fig. 10 TG–DTG curve of PIB–OH.

Fig. 10 shows the TG–DTG curve. A slight decrease was observed during the heating stage of 40 °C–380 °C because of the solvent residue that escaped incompletely in the product. After that, the thermal decomposition temperature of PIB–OH was higher than 380 °C, and it could be completely decomposed without residue. This finding indicates that the material had excellent thermal stability.

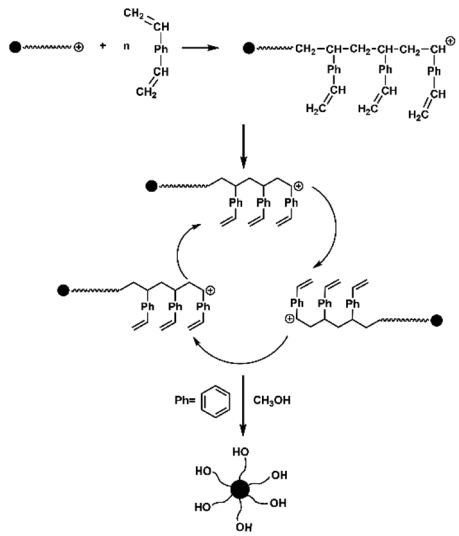

Fig. 11 Synthesis route of star-shaped telechelic PIB.

3.2 Synthesis of star-shaped telechelic PIB

Fig. 11 shows the synthesis route of star-shaped telechelic PIB. First, the living chain of PIB was synthesized by the living cationic polymerization system. Next, it followed by the addition of a divinyl compound crosslinker, which was used as the "nucleus" to react with the arm chain. The final forms the hydroxy head group of the polymer arm chain after the termination reaction. Therefore, we innovatively synthesized well-defined star-shaped hydroxy-terminal PIB by using arm-core method.

DVB is an effective crosslinking agent with high reactivity. So it can be used to synthesize star-shaped PIB structures quantitatively. The influence of DVB dosage on the reaction has been studied. As shown in Table 3, the initiator to DVB ratio (r) (r = [PO]/[DVB]), arm chain length, reaction time, have a significantly impact on the cross-linking reaction. The Mw was determined by MALLS and average number (N) of arms per star-shaped polymer calculated from Mw.[44]

The detailed experimental results are shown in Table 3. In the experiment, the arm chain with higher molecular weight had large steric hindrance in the system. This large steric hindrance effect slowed down the connection between the arms and inhibited the coupling between the star parts effectively. The average number of arm star-shaped polymer reaches 5.8 at 60 min of reaction. The system does not appear to gel even when the r value is low (Table 3, entry 1). The coupling rate between the arm chains was accelerated when the smaller molecular weight arm chains were nucleated with divinylbenzene. The star-shaped part of the reaction was basically completed in 2 min. This time allows the star-shaped polymer to be formed quickly and quantitatively, with no gel generated in the system at this time. The average number of arms N and the Mw of star-shaped polymers increased with the cross-linking agent DVB feed ratio. The average number of arms can reach 1.6 when r = 3.2 (Table 3, entry 7). At the same time, we can see that the molecular weight distribution increases as r increases due to the formation of star structures.

Table 3 Characterization of star-shaped PIB obtained with DVB[a]

entry	r	Linking time (min)	Arm chain Mw (g mol^{-1})	Star-shaped part Mw (g mol^{-1})	Mw/Mn	N
1	0.2 : 1	60	22 744	132 680	1.46	5.8
2	4.0 : 1	2	5290	7940	1.60	1.5
3		4		9550	1.63	1.8
4		6		15 500	1.82	2.9
5	3.4 : 1	2	4775	7154	1.59	1.5
6		4		16 120	2.80	3.3
7	3.2 : 1	2	10 370	16 560	1.38	1.6
8	2.9 : 1	2	4704	7712	1.57	1.6
9		4		18 110	3.91	3.8

[a] Reaction conditions: T = −80 °C, [$TiCl_4$] : [PO] = 2 : 1, [DTBP] = 0.01 M, r = 0.2, 2.9, 3.2, 3.4, 4.0, linking time = 2, 4, 6, 60 min.

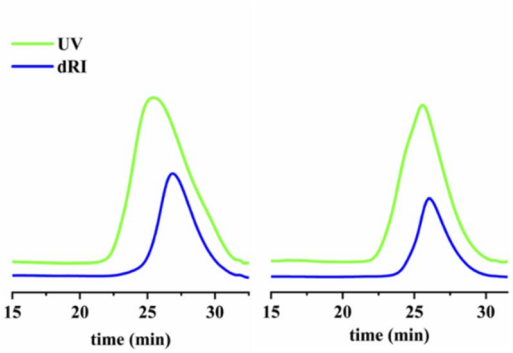

Fig. 12 Star polymer of UV and RI signal as a function of elution time. Linking reaction: $T = -80$ °C; Hex/MeCl = 6/4 (v/v); linking time = 2 min.

Fig. 12 shows the UV and RI signal as a function of elution time of star polymers. (More curves can been found in Fig. S1†). Compared with IB homopolymers, star polymers have UV absorption peaks, indicating that the macromolecular chain contains benzene ring UV absorption groups. The UV elution curve is consistent with the peak time of the differential elution curve. This indicated that the divinyl compound crosslinking agent enters the chain successfully, and the star structure has been generated.

The structure of the star polymer has been characterized by ^{1}H-NMR. Fig. 13 shows the ^{1}H-NMR spectrum of star-shaped end-hydroxy PIB. In comparison with the ^{1}H-NMR spectrum of linear end-hydroxy PIB, the proton resonances at $\delta = 6.6$–7.5 ppm correspond to the benzene ring protons (a). The DVB in the reaction system did not completely react with some double bonds that remained in the residue. The proton resonances at $\delta = 5.70$ ppm correspond to $=CH_2$ (c), and the proton resonances at $\delta = 5.20$ ppm correspond to –CH= (b). The proton resonances at $\delta = 3.31$ ppm (peak d′) and $\delta = 3.48$ ppm (peak d) correspond to the methylene protons that are next to the primary hydroxyl head group, and these two protons split because the neighboring protons are chiral. This result indicated that the hydroxyl PIB chain was successfully grafted to the nuclear structure. The product contained a star-shaped macromolecular structure with DVB as the nucleus. According to previous characterization studies of linear polymer, hydroxyl is quantitative. Therefore, each arm chain of star polymer contains hydroxyl group, which is also quantitative.

The relationship of between molecular radius of rotation (Rg) and molar mass (M) can also reflect the information of molecular structure. It can be used as a benchmark to qualitatively determine the structure of branched polymer or star polymer. The curve of the Rg and M can be plotted from the data of MALLS. The plot can fit into a linear shape. The slope indicates the degree of molecular branching. The Rg and M have the following relationship: $Rg = K' \cdot M^{\alpha}$, α is expressed as the slope in the graph. The degree of branching of the polymer chains can be determined by the branching factor. The smaller the α value is, the higher the branching degree of polymer will be.[45,46] As shown in Fig. 14, the index of linear hydroxy-terminated PIB was $\alpha = 0.67$. The polymer was in the linear random coils configuration in the solvent. In contrast, the star-shaped hydroxy-terminated PIB performed an index of $\alpha = 0.15$. It is a spherical conformation in dilute solution. This finding confirms the successful synthesis of the star-shaped telechelic PIB.

Previously, we have discussed the case of star polymers synthesized from high molecular weight arm chains. Notably, the low molecular weight arm chains have a low spatial site resistance. When used it for the synthesis of star polymer, the possibility of interconnection between the primary star parts already formed in the early stages of the reaction increased.[44] Thus, as the cross-linking reaction time increases, the star–star coupling among multiple nuclei begins to occur (Table 3, entries 3, 4, 6, 9). It leads to the depletion of coupling sites in the system. Therefore, the molecular weight of the lower molecular region no longer increases, and the primary star polymer is no longer formed.

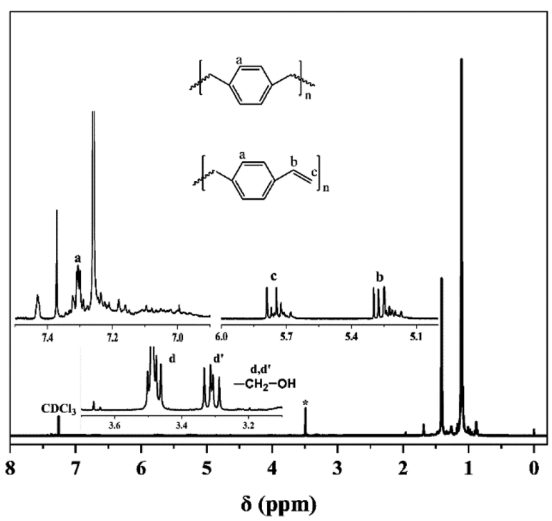

Fig. 13 ^{1}H-NMR spectrum of star-shaped PIB.

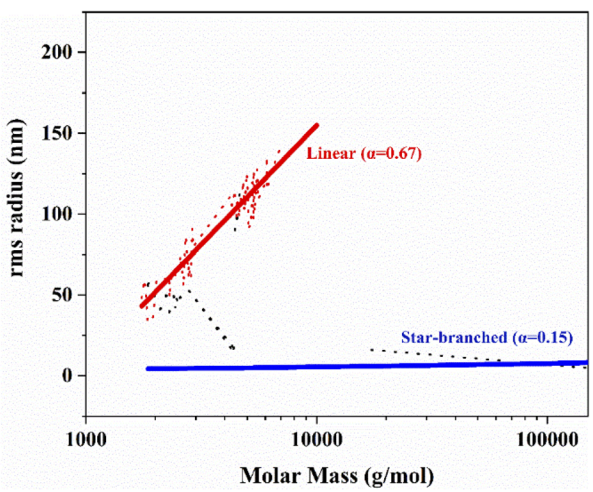

Fig. 14 The relationship between log Rg and log M.

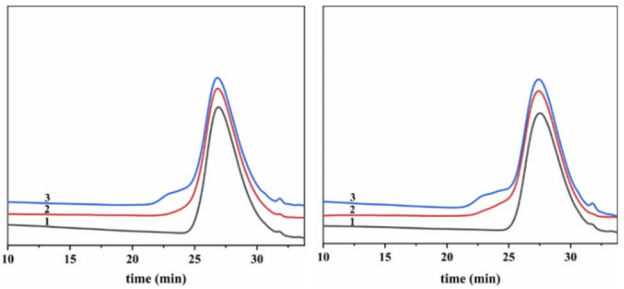

Fig. 15 RI signal as a function of elution time at different coupling reaction times. Linking time min^{-1}: 1–0 min, 2–2 min, 3–4 min; T = −80 °C; Hex/MeCl = 6/4 (v/v).

Next, we conducted the MALLS test of star-shaped polymers. Fig. 15 shows star-shaped polymer RI signal as a function of elution time at different coupling reaction times. (More curves can been found in Fig. S2†). The peak position of the differential curve moves forward with the extension of coupling time. A distinct shoulder peak was observed at 4 min of coupling reaction in all cases. Fig. 16 shows the light scattering intensity as a function of elution time of star polymers (Table 3, entry 9). The laser signal shows obvious double peaks, and signs of double peaks are observed in the forward shift of the UV curve. This is the interconnection of primary star polymers that contain benzene ring cross-linkers. The final resulted in the generation of ultra-high molecular weight branched polymers, thereby proving the occurrence of star–star coupling phenomenon.

The signal intensity of the differential signal is proportional to the concentration of each component in the polymer. By peak-differentiating and fitting analysis, we calculate the proportion of ultra-high molecular weight cross-linked core (Fig. 17). The proportion reached 6.6%, the final product also showed that the gel state cannot dissolve. This also confirmed

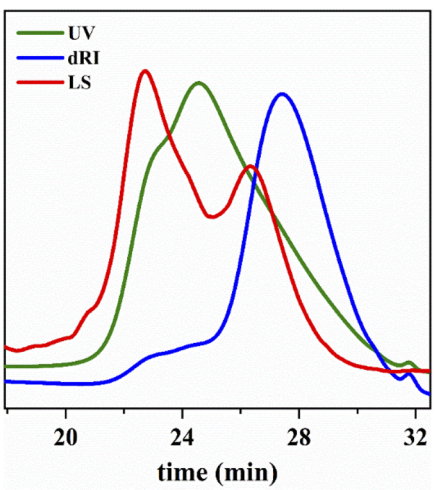

Fig. 16 Light scattering intensity as a function of elution time.

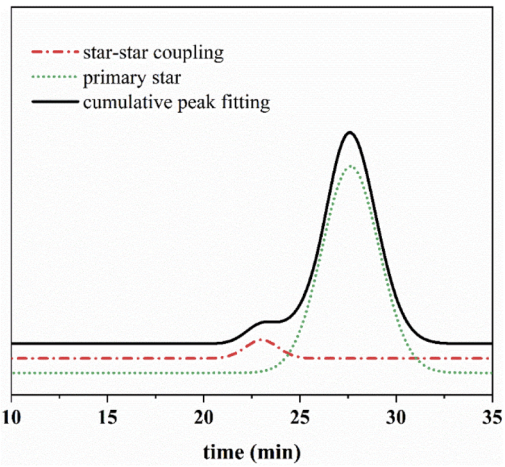

Fig. 17 Split-peak fitting of the differential signal.

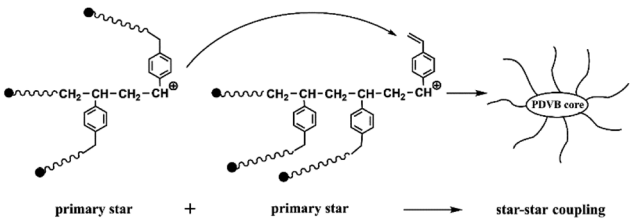

Fig. 18 Star–star linkage reaction.

that the linkage between star–star portions does occur in primary star polymers prepared from low molecular weight arm chains as the coupling time increases. Finally, a cross-linked nucleus was formed. Therefore, the coupling time should not be too long when using low molecular weight arm chains for the preparation of star-shaped telechelic polymer in this reaction system.

Through the above experimental exploration, we speculated the formation of cross-linked nuclei. As shown in Fig. 18, the star–star linkage reaction in the cationic polymerization system is depicted as the coupling time increases. The PIB–DVB$^{\oplus}$ cation at the end of the primary star polymer living chain reacts with the side chain vinyl (–CH═CH$_2$) group in the PIB–DVB. The results show the formation of ultra-high molecular weight cross-linked nuclei and the appearance of gelation.

The final results show that regardless of the arm chain length, we can optimize the reaction conditions so that the arm chains can react with the crosslinker effectively to form star-shaped polymer. This result also confirms the feasibility of fast and quantitative synthesis of star-shaped hydroxy-terminated PIB by one-pot method of cationic polymerization, thereby providing a good strategy for the preparation of star-shaped polymer with specific functional groups.

4 Conclusions

In this paper, the hydroxyl-terminated PIB has been successfully synthesized by living cationic polymerization using PO/TiCl$_4$ as

functionalized initiator system. The ^{1}H-NMR results confirmed the polymer structure and combined with Gaussian simulations verified the proposed polymerization mechanism. The preparation of star-shaped hydroxy-terminated PIB was also successfully achieved by the addition of divinylbenzene cross-linker. It was found that when high molecular weight arm chains were used, the coupling phenomenon between the star-shaped parts could be effectively suppressed. When low molecular weight arm chains were used, coupling between the stars occurred after 4 min reaction time even with a low concentration of cross-linking agent, and the significant gelation phenomenon appeared.

Conflicts of interest

The authors declare no conflicts of interest.

Acknowledgements

This research was funded by the National Natural Science Foundation of China (No. 52073033), Beijing Excellent Talents Training Fund (No. Z2019-042), Petrochina Company Limited Lanzhou Chemical Research Center Research Fund (No. KYWX-21–014), Beijing Institute of Petrochemical Technology URT Program (NO. 2022J00047).

References

1 T. Takeda, *Nippon Gomu Kyokaishi*, 2005, **78**, 78–80.
2 J. V. Fusco and P. Hous, *Rubber Technol.*, 1987, 284–321.
3 D. I. Shiman, I. A. Berezianko and I. V. Vasilenko, *Chin. J. Polym. Sci.*, 2019, **37**, 891–897.
4 S. Yuan, Z. Li and L. Song, *ACS Appl. Mater. Interfaces*, 2016, **8**, 21214–21220.
5 T. Kwee, S. J. Taylor and K. A. Mauritz, *Polymer*, 2005, **46**, 4480–4491.
6 E. Ovcharenko, M. Rezvova and P. Nikishau, *Appl. Sci.*, 2019, **9**, 4773.
7 J. Sheriff, T. E. Claiborne and P. L. Tran, *ACS Appl. Mater. Interfaces*, 2015, **7**, 22058–22066.
8 N. C. Kekec, M. B. Akolpoglu and U. Bozuyuk, *Polym. Adv. Technol.*, 2019, **30**, 1836–1846.
9 L. Pinchuk, G. J. Wilson and J. J. Barry, *Biomaterials*, 2008, **29**, 448–460.
10 J. Kennedy and B. Ivan, *Designed Polymers by Carbocationic Macromolecular Engineering*, Hanser Publishers, Munich, New York, 1992.
11 B. Iván, I. Szanka and Á. Szabó, *Macromolecular Engineering*, Amsterdam, 2021, 23–49.
12 Y. Kwon, R. Faust and C. X. Chen, *Macromolecules*, 2002, **35**, 3348–3357.
13 Z. Fang and J. P. Kennedy, *J. Polym. Sci., Part A: Polym. Chem.*, 2002, **40**, 3662–3678.
14 T. Higashihara, D. Feng and R. Faust, *Macromolecules*, 2006, **39**, 5275–5279.
15 A. Takacs and R. Faust, *Macromolecules*, 1995, **28**, 7266–7270.
16 H. Everland, J. Kops and A. Nielsen, *Polym. Bull.*, 1993, **31**, 159–166.
17 B. Iván, X. Chen and J. Kops, *Macromol. Rapid Commun.*, 1998, **19**, 15–19.
18 X. Chen, B. Iván and J. Kops, *Macromol. Rapid Commun.*, 1998, **19**, 585–589.
19 J. Feldthusen, B. Iván and A. H. E. Müller, *Macromolecules*, 1998, **31**, 578–585.
20 Á. Szabó, G. Szarka and B. Iván, *Macromol. Rapid Commun.*, 2015, **36**, 238–248.
21 Á. Szabó, A. Wacha and R. Thomann, *J. Macromol. Sci., Part A: Pure Appl.Chem.*, 2015, **52**, 252–259.
22 B. Kerscher, T. M. Trötschler and B. Pásztói, *Macromolecules*, 2019, **52**, 3306–3318.
23 B. Pásztói, T. M. Trötschler and Á. Szabó, *Polymers*, 2020, **12**, 2504.
24 K. Ren, M. Zhang and J. He, *ACS Appl. Mater. Interfaces*, 2015, **7**, 11263–11271.
25 Y. Wang and M. A. Hillmyer, *Polym. Chem.*, 2015, **6**, 6806–6811.
26 J. Kang, G. Erdodi and J. P. Kennedy, *J. Polym. Sci., Part A: Polym. Chem.*, 2011, **49**, 3891–3904.
27 B. Iván, K. Almdal and K. Mortensen, *Macromolecules*, 2001, **34**, 1579–1585.
28 G. Erdödi and B. Iván, *Chem. Mater.*, 2004, **16**, 959–962.
29 B. Iván, M. Haraszti and G. Erdődi, *Macromol. Symp.*, 2005, **227**, 265–274.
30 M. Haraszti, E. Tóth and B. Iván, *Chem. Mater.*, 2006, **18**, 4952–4958.
31 S. Pásztor, B. Iván and G. Kali, *J. Polym. Sci., Part A: Polym. Chem.*, 2017, **55**, 1818–1821.
32 S. Pásztor, B. Becsei and G. Szarka, *Materials*, 2020, **13**, 4822.
33 B. Ivan, J. P. Kennedy and V. S. C. Chang, *J. Polym. Sci., Polym. Chem. Ed.*, 1980, **18**, 3177–3191.
34 J. P. Kennedy, B. Ivan and V. S. C. Chang, *Urethane Chemistry and Applications*, 1981, 25, 383–391.
35 J. P. Kennedy, V. S. Chang, R. A. Smith and B. Iván, *Polym. Bull.*, 1979, 575–580.
36 B. Ivan and J. P. Kennedy, *J. Polym. Sci., Part A: Polym. Chem.*, 1990, **28**, 89–104.
37 U. Ojha, R. Rajkhowa, S. R. Agnihotra and R. Faust, *Macromolecules*, 2008, **41**, 3832–3841.
38 W. Kangda, W. Yibo and S. Huang, *RSC Adv.*, 2020, **10**, 9601–9609.
39 A. J. D. Magenau, J. W. Chan and C. E. Hoyle, *Polym. Chem.*, 2010, **1**, 831–833.
40 Li Jing, W. Kang-Da and S. Huang, *Chin. J. Polym. Sci.*, 2019, **37**, 936–942.
41 J. E. Puskas, S. H. Soytaş and G. T. Lim, *Macromol. Symp.*, 2011, **308**, 61–67.
42 Q. Yan, X. Sui and J. Yuan, *Prog. Chem.*, 2008, **20**, 1562–1571.
43 T. Higashihara, M. Hayashi and A. Hirao, *Prog. Polym. Sci.*, 2011, **36**, 323–375.
44 T. Yoshizaki, A. Kanazawa and S. Kanaoka, *Macromolecules*, 2016, **49**, 71–79.
45 L. Zhang, Y. Wu and S. Li, *Acta Polym. Sin.*, 2015, **9**, 1028–1035.
46 T. M. Marsalkó, I. Majoros and J. P. Kennedy, *Macromol. Symp.*, 1995, **95**, 39–56.